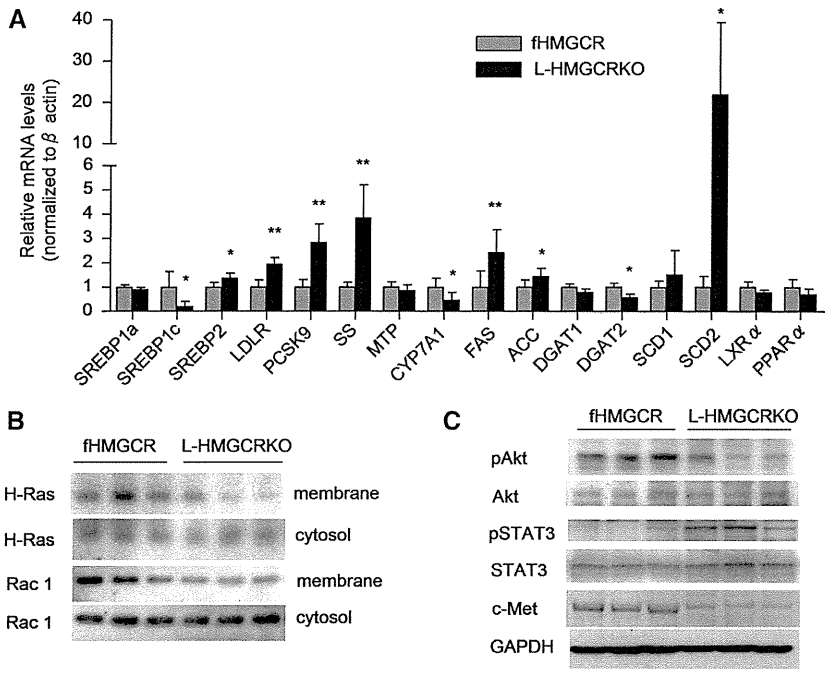

Figure 4. Relative amounts of various mRNAs and degree of isoprenylation of small GTP-binding proteins and liver regeneration-associated proteins in the livers of control and liver-specific HMGCR knockout (L-HMGCRKO) male mice at 4 weeks of age. **A**, Total RNA from the livers of mice (n=5 in each group) was subjected to quantitative real-time polymerase chain reaction as described in the online-only Data Supplement. Each value represents the amount of mRNA relative to that in the control mice, which is arbitrarily defined as 1. **B**, Liver membranous and cytosolic fractions for small GTP-binding proteins or (**C**) liver tissue lysates for liver regeneration-associated proteins were prepared as described in the online-only Data Supplement (n=3 in each group), and aliquots (30 μg) were subjected to SDS-PAGE and immunoblot analysis. Each value represents mean±SD. Significant differences compared with control mice: **P*<0.05 and ***P*<0.01. LDLR indicates low-density lipoprotein receptor; PCSK9, proprotein convertase subtilisin/kexin type 9; FAS, fatty acid synthase; DGAT, diacylglycerol acyltransferase; SCD, stearoyl-CoA desaturase; LXR α, liver X receptor; PPARα, peroxisome proliferator–activated receptor α; SS, squalene synthase; MTP, microsomal triglyceride transfer protein; CYP7A1, cholesterol 7α-hydroxylase; ACC, acetyl-CoA carboxylase; GAPDH, glyceraldehyde-3-phosphate dehydrogenase; STAT3, signal transducer and activator of transcription 3.

to the hepatic toxicity and hypoglycemia. Unexpectedly, the mice developed hypercholesterolemia before death, although hepatic cholesterol synthesis was significantly reduced. This lethal phenotype was completely reversed by mevalonate or glucose, indicating that mevalonate is essential for the survival of mice and that hypoglycemia is the direct cause of lethality.

The mRNA expression of HMGCR was reduced as early as 3 weeks of age and almost undetectable at 4 weeks. This developmental reduction in the expression is consistent with the developmental induction of the expression of albumin. Other liver-specific KO models using Alb-Cre showed abrogation of the expression of reporter genes at a similar stage.[12] However, the HMGCR activity of the liver was reduced by only 50%. Because the parenchymal hepatocytes from the liver of the L-HMGCRKO mice at 3 weeks of age expressed substantial HMGCR activity, we speculate that most of the activity is derived from upregulated HMGCR expression in a certain subset of hepatocytes that escaped from HMGCR gene inactivation. Indeed, recombination efficiency was only 75% at weaning,[13] and HMGCR protein can be increased 25-fold at the posttransciptional level.[1]

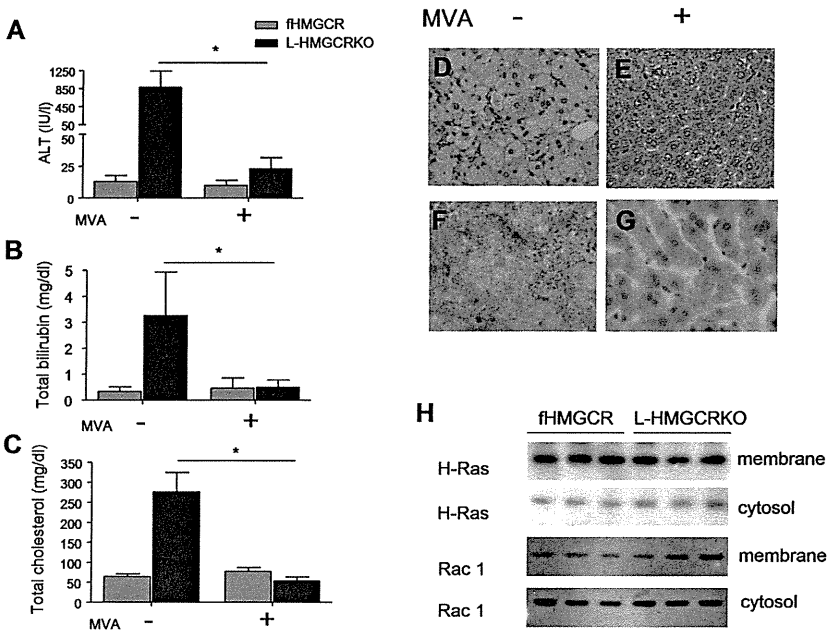

Figure 5. Supplementation of mevalonate. Male mice were given mevalonate in drinking water at a concentration of 5 mmol/L from the age of 28 days to 35 days (n=5 in each group). After supplementation, plasma alanaine transaminase (ALT) (**A**), total bilirubin (**B**), and total cholesterol (**C**) levels were measured. The livers were removed from liver-specific HMGCR knockout (L-HMGCRKO) mice not supplemented with mevalonate (–; **D** and **F**, respectively) or supplemented with mevalonate (+; **E** and **G**, respectively) stained with hematoxylin and eosin or oil-red O. **H**, Immunoblot analyses for small GTP-binding proteins in membranous and cytosolic fractions of the liver. Each value represents mean±SD. Significant differences compared with control mice: **P*<0.001.

Furthermore, there might be time lag between disappearance of HMGCR protein and cessation of transcription.

Sex dimorphism in lethality is noteworthy. The present results that male L-HMGCRKO mice were more prone to die than females are consistent with the general view that females are more resistant to morbidity and mortality of various liver diseases than males.[14] In addition to protection against liver injury via vasodilating and anti-inflammatory effects, estrogen itself attenuates the development of hepatic steatosis.[15] The mRNA expression levels of HMGCR in the liver of the surviving L-HMGCRKO mice were indistinguishable from those of fHMGCR mice (Figure IIB in the online-only Data Supplement). It is likely that the hepatocytes with a relatively intact HMGCR gene may be extensively regenerated, thereby eventually compensating for the KO in the survivors. In support of this, several Ki-67–positive cells were greatly increased in the L-HMGCRKO mice (Figure 2L and 2N).

Hepatic cholesterol levels were mildly decreased, and the decrease in plasma cholesterol levels was modest in the L-HMGCRKO mice at 3 weeks of age. More surprisingly, the plasma cholesterol levels even increased immediately before death. Extrahepatic organs with high cholesterol synthesis, such as skin, bowels, and muscles, may be a source of cholesterol in the plasma.[16] The hypercholesterolemia before death appears paradoxical, given the failure of cholesterol synthesis in the hepatocytes. At this stage, the mice develop jaundice. Because the physicochemical characteristics of the accumulated lipoproteins were similar to those of lipoprotein X, cholestasis may at least partly account for hypercholesterolemia. Simultaneous accumulation of both lipoprotein X and apoB48-containing particles has also been reported in rats with intrahepatic cholestasis.[17]

Interestingly, L-HMGCRKO mice showed hepatic steatosis. Because hepatic triglyceride levels were increased 2-fold but hepatic cholesterol ester levels were not increased (data not shown) most of the neutral lipids stained with oil-red O are triglycerides. Supporting this, the synthesis of fatty acids was increased 17-fold. In this context, it is noteworthy that the expression of enzymes for fatty acid synthesis, FAS and stearoyl-CoA desaturase 2, was increased. In normal adults, stearoyl-CoA desaturase 1 is the major enzyme catalyzing desaturation of oleate, whereas stearoyl-CoA desaturase 2 is an isozyme that is transiently expressed in the liver in embryos and neonates and may be involved in lipogenesis at that developmental stage.[18] Indeed, the amounts of polyunsaturated fatty acids were increased in the liver (Figure 3F).

The increase in fatty acids synthesis appeared disproportionately larger than the increase in triglycerides in the liver. In this context, it is of note that the expression of diacylglycerol acyltransferase 1 was not increased and that of diacylglycerol acyltransferase 2 was even decreased. Thus, it is probable that the newly synthesized fatty acids were not used to produce triglycerides. Generally, the enzymes catalyzing fatty acid synthesis are transcriptionally induced by SREBP1c. However, the expression of SREBP1c was reduced 5-fold, suggesting that the increased lipogenesis was not mediated by SREBP1c. Similar SREBP1c-independent lipogenesis is reported in mice overexpressing a constitutively active form of Akt in the liver.[19] Furthermore, the levels of LXRα mRNA, a nuclear receptor that can stimulate SREBP1c gene expression[20] and can also directly stimulate transcription of FAS,[21] were not increased in the livers of L-HMGCRKO mice. We speculate that the lack of cholesterol reduces the supply of oxysterols, physiological ligands of LXR, which transactivates SREBP1c.[22] This notion is supported by the decreased expression of cholesterol 7α-hydroxylase and diacylglycerol acyltransferase 2, also targets of LXR.

In contrast to SREBP1c expression, the expression of SREBP2 was increased, conceivably accounting for the increased expression of its targets: the LDL receptor and squalene synthase. The expression of FAS in the face of significant suppression of SREBP1c or unaltered LXRα suggests a regulatory pathway independent of SREBP1c or LXRα. Recently, a decrease in farnesyl pyrophosphate or farnesol has been shown to induce the expression of FAS independently of SREBP1c.[23]

The liver of the L-HMGCRKO mice contained increased numbers of TdT-mediated dUTP-nick end labeling–positive cells. Consistent with the apoptotic nature of the cell death, the activity of caspase 3, a final executer of apoptosis which cleaves to induce the release of cytochrome c from mitochondria, was increased in the liver of the L-HMGCRKO mice. We have hypothesized several potential mechanisms for apoptosis: accumulation of toxic lipid metabolites[24] and reduction of survival factors.[25] However, we failed to obtain evidence for the involvement of ceramide and survivin in apoptosis.

As predicted, membrane-bound forms of Ras and Rac1 were significantly reduced, conceivably as a result of the defect in their isoprenylation. Several mechanisms linking the defect in isoprenylation to apoptosis have been proposed. For example, Rac1 is reported to protect against apoptosis by stimulating nicotinamide adenine dinucleotide phosphate-oxidase, thereby increasing the levels of reactive oxygen species.[26] However, we failed to detect a decrease in H_2O_2 levels in the liver.

During the search for the plausible mechanism of the hepatocyte apoptosis, we found a significant increase in the mRNA level of C/EBP-homologous protein, a hallmark of the ER stress response and inducer of apoptosis, in the liver of L-HMHCRKO mice. Because hepatic steatosis induces ER stress, it is reasonable to speculate that the increased synthesis of fatty acids causes hepatic lipoapoptosis via increasing the C/EBP-homologous protein. The liver of L-HMGCRKO mice had significantly decreased levels of either p-Akt or c-met protein. Because hepatocyte growth factor exerts prosurvival effects mainly through activating phosphatidylinositol-3 kinase/Akt pathway after binding to its receptor, c-met,[27] defective hepatocyte growth factor signaling may play a salutary role in the induction of hepatocyte apoptosis. The increase in phospho-signal transducer and activator of transcription 3 might be a compensatory response secondary to increased apoptosis, but failed to overcome it. Similar failure to compensate the liver failure by activated signal transducer and activator of transcription 3 was reported in mice deficient in phosphoinositide-dependent protein kinase 1.[28]

These phenotypes of L-HMGCRKO mice should be discussed in relation to other mouse models of genetic disorders of cholesterol metabolism. Thus far, 2 models have been reported to survive the perinatal period, despite reduced cholesterol biosynthesis in the liver. Because the global disruption of SREBP cleavage-activating protein and site 1 protease is embryonic lethal, as is the case for HMGCR, liver-specific KO

mice have been generated. In both the liver-specific SREBP cleavage-activating protein[29] and site 1 protease KO mice,[30] the synthesis of cholesterol as well as fatty acids was significantly reduced in the liver. Neither mouse, however, died of liver toxicity, probably because the reduction in the expression of HMGCR was not as severe as in L-HMGCRKO mice.

In conclusion, HMGCR is essential for the survival of mice. Despite the defect in hepatic cholesterol biosynthesis in L-HMGCRKO mice, the homeostasis of cholesterol in the liver and plasma is surprisingly well maintained presumably via compensatory changes in the flux of cholesterol and fatty acids. These results might provide insight for understanding the role of cholesterol biosynthetic pathway in the normal function of hepatocytes.

Acknowledgments

We thank Drs Derek LeRoith, Wataru Ogawa, and Masato Kasuga for providing Alb-Cre mice. We also thank Drs Tetsuya Kitamine, Ryuichi Tozawa, Yoshiaki Tamura, Hiroaki Okazaki, Masaki Igarashi, Hitoshi Shimano, and Nobuhiro Yamada for their help and discussion.

Sources of Funding

This work was supported by a Grant-in-Aid for Scientific Research from the Ministry of Education, Science and Culture and the Program for Promotion of Fundamental Studies in Health Sciences of the National Institute of Biomedical Innovation (NIBIO) and JKA through its promotion funds from KEIRIN RACE.

Disclosures

None.

References

1. Goldstein JL, Brown MS. Regulation of the mevalonate pathway. *Nature*. 1990;343:425–430.
2. Liscum L, Finer-Moore J, Stroud RM, Luskey KL, Brown MS, Goldstein JL. Domain structure of 3-hydroxy-3-methylglutaryl coenzyme A reductase, a glycoprotein of the endoplasmic reticulum. *J Biol Chem*. 1985;260:522–530.
3. Hua X, Nohturfft A, Goldstein JL, Brown MS. Sterol resistance in CHO cells traced to point mutation in SREBP cleavage-activating protein. *Cell*. 1996;87:415–426.
4. Sever N, Yang T, Brown MS, Goldstein JL, DeBose-Boyd RA. Accelerated degradation of HMG CoA reductase mediated by binding of insig-1 to its sterol-sensing domain. *Mol Cell*. 2003;11:25–33.
5. Kathiresan S, Melander O, Guiducci C, Surti A, Burtt NP, Rieder MJ, Cooper GM, Roos C, Voight BF, Havulinna AS, Wahlstrand B, Hedner T, Corella D, Tai ES, Ordovas JM, Berglund G, Vartiainen E, Jousilahti P, Hedblad B, Taskinen MR, Newton-Cheh C, Salomaa V, Peltonen L, Groop L, Altshuler DM, Orho-Melander M. Six new loci associated with blood low-density lipoprotein cholesterol, high-density lipoprotein cholesterol or triglycerides in humans. *Nat Genet*. 2008;40:189–197.
6. Endo A, Kuroda M, Tanzawa K. Competitive inhibition of 3-hydroxy-3-methylglutaryl coenzyme A reductase by ML-236A and ML-236B fungal metabolites, having hypocholesterolemic activity. *FEBS Lett*. 1976;72:323–326.
7. Baigent C, Keech A, Kearney PM, Blackwell L, Buck G, Pollicino C, Kirby A, Sourjina T, Peto R, Collins R, Simes R; Cholesterol Treatment Trialists' (CTT) Collaborators. Efficacy and safety of cholesterol-lowering treatment: prospective meta-analysis of data from 90,056 participants in 14 randomised trials of statins. *Lancet*. 2005;366:1267–1278.
8. Liao JK, Laufs U. Pleiotropic effects of statins. *Annu Rev Pharmacol Toxicol*. 2005;45:89–118.
9. Ohashi K, Osuga J, Tozawa R, Kitamine T, Yagyu H, Sekiya M, Tomita S, Okazaki H, Tamura Y, Yahagi N, Iizuka Y, Harada K, Gotoda T, Shimano H, Yamada N, Ishibashi S. Early embryonic lethality caused by targeted disruption of the 3-hydroxy-3-methylglutaryl-CoA reductase gene. *J Biol Chem*. 2003;278:42936–42941.
10. Tozawa R, Ishibashi S, Osuga J, Yagyu H, Oka T, Chen Z, Ohashi K, Perrey S, Shionoiri F, Yahagi N, Harada K, Gotoda T, Yazaki Y, Yamada N. Embryonic lethality and defective neural tube closure in mice lacking squalene synthase. *J Biol Chem*. 1999;274:30843–30848.
11. Yakar S, Liu JL, Stannard B, Butler A, Accili D, Sauer B, LeRoith D. Normal growth and development in the absence of hepatic insulin-like growth factor I. *Proc Natl Acad Sci USA*. 1999;96:7324–7329.
12. Inoue H, Ogawa W, Ozaki M, Haga S, Matsumoto M, Furukawa K, Hashimoto N, Kido Y, Mori T, Sakaue H, Teshigawara K, Jin S, Iguchi H, Hiramatsu R, LeRoith D, Takeda K, Akira S, Kasuga M. Role of STAT-3 in regulation of hepatic gluconeogenic genes and carbohydrate metabolism in vivo. *Nat Med*. 2004;10:168–174.
13. Postic C, Magnuson MA. DNA excision in liver by an albumin-Cre transgene occurs progressively with age. *Genesis*. 2000;26:149–150.
14. Yokoyama Y, Nimura Y, Nagino M, Bland KI, Chaudry IH. Current understanding of gender dimorphism in hepatic pathophysiology. *J Surg Res*. 2005;128:147–156.
15. Nemoto Y, Toda K, Ono M, Fujikawa-Adachi K, Saibara T, Onishi S, Enzan H, Okada T, Shizuta Y. Altered expression of fatty acid-metabolizing enzymes in aromatase-deficient mice. *J Clin Invest*. 2000;105:1819–1825.
16. Spady DK, Dietschy JM. Sterol synthesis in vivo in 18 tissues of the squirrel monkey, guinea pig, rabbit, hamster, and rat. *J Lipid Res*. 1983;24:303–315.
17. Chisholm JW, Dolphin PJ. Abnormal lipoproteins in the ANIT-treated rat: a transient and reversible animal model of intrahepatic cholestasis. *J Lipid Res*. 1996;37:1086–1098.
18. Miyazaki M, Dobrzyn A, Elias PM, Ntambi JM. Stearoyl-CoA desaturase-2 gene expression is required for lipid synthesis during early skin and liver development. *Proc Natl Acad Sci USA*. 2005;102:12501–12506.
19. Ono H, Shimano H, Katagiri H, Yahagi N, Sakoda H, Onishi Y, Anai M, Ogihara T, Fujishiro M, Viana AY, Fukushima Y, Abe M, Shojima N, Kikuchi M, Yamada N, Oka Y, Asano T. Hepatic Akt activation induces marked hypoglycemia, hepatomegaly, and hypertriglyceridemia with sterol regulatory element binding protein involvement. *Diabetes*. 2003;52:2905–2913.
20. Chen G, Liang G, Ou J, Goldstein JL, Brown MS. Central role for liver X receptor in insulin-mediated activation of Srebp-1c transcription and stimulation of fatty acid synthesis in liver. *Proc Natl Acad Sci USA*. 2004;101:11245–11250.
21. Joseph SB, Laffitte BA, Patel PH, Watson MA, Matsukuma KE, Walczak R, Collins JL, Osborne TF, Tontonoz P. Direct and indirect mechanisms for regulation of fatty acid synthase gene expression by liver X receptors. *J Biol Chem*. 2002;277:11019–11025.
22. Yoshikawa T, Shimano H, Amemiya-Kudo M, Yahagi N, Hasty AH, Matsuzaka T, Okazaki H, Tamura Y, Iizuka Y, Ohashi K, Osuga J, Harada K, Gotoda T, Kimura S, Ishibashi S, Yamada N. Identification of liver X receptor-retinoid X receptor as an activator of the sterol regulatory element-binding protein 1c gene promoter. *Mol Cell Biol*. 2001;21:2991–3000.
23. Murthy S, Tong H, Hohl RJ. Regulation of fatty acid synthesis by farnesyl pyrophosphate. *J Biol Chem*. 2005;280:41793–41804.
24. Anderson N, Borlak J. Molecular mechanisms and therapeutic targets in steatosis and steatohepatitis. *Pharmacol Rev*. 2008;60:311–357.
25. Kaneko R, Tsuji N, Asanuma K, Tanabe H, Kobayashi D, Watanabe N. Survivin down-regulation plays a crucial role in 3-hydroxy-3-methylglutaryl coenzyme A reductase inhibitor-induced apoptosis in cancer. *J Biol Chem*. 2007;282:19273–19281.
26. Deshpande SS, Angkeow P, Huang J, Ozaki M, Irani K. Rac1 inhibits TNF-alpha-induced endothelial cell apoptosis: dual regulation by reactive oxygen species. *FASEB J*. 2000;14:1705–1714.
27. Xiao GH, Jeffers M, Bellacosa A, Mitsuuchi Y, Vande Woude GF, Testa JR. Anti-apoptotic signaling by hepatocyte growth factor/Met via the phosphatidylinositol 3-kinase/Akt and mitogen-activated protein kinase pathways. *Proc Natl Acad Sci USA*. 2001;98:247–252.
28. Haga S, Ozaki M, Inoue H, Okamoto Y, Ogawa W, Takeda K, Akira S, Todo S. The survival pathways phosphatidylinositol-3 kinase (PI3-K)/phosphoinositide-dependent protein kinase 1 (PDK1)/Akt modulate liver regeneration through hepatocyte size rather than proliferation. *Hepatology*. 2009;49:204–214.
29. Matsuda M, Korn BS, Hammer RE, Moon YA, Komuro R, Horton JD, Goldstein JL, Brown MS, Shimomura I. SREBP cleavage-activating protein (SCAP) is required for increased lipid synthesis in liver induced by cholesterol deprivation and insulin elevation. *Genes Dev*. 2001;15:1206–1216.
30. Yang J, Goldstein JL, Hammer RE, Moon YA, Brown MS, Horton JD. Decreased lipid synthesis in livers of mice with disrupted Site-1 protease gene. *Proc Natl Acad Sci USA*. 2001;98:13607–13612.

Supplemental material

Supplemental Methods

Generation of mice heterozygous for the floxed HMGCR allele

A conditional targeting vector of a replacement type was produced by inserting a loxP site into a XhoI site in intron 1 and loxP-flanked (floxed) polII-neo-bpA cassette into a BamHI site in intron 4 (Supplemental figure I). The transcriptional orientation of the neo gene was opposite to that of the HMGCR gene. Excision of sequences between the loxP sites by Cre recombinase deletes exons 2 to 4, which includes the initiator methionine and residues encoding the first membrane-bound domain of HMHCR. JH1 ES cells (A gift from Dr. J. Herz) were electroporated with the targeting vector as described[1]. Recombinant clones containing a single floxed HMGCR allele were identified by PCR using primers primers P1 (5'-ACGAAAGGGCCTCGTGATACGCCTA-3') and P2 (5'-ATGTCTGCAGTCCCAGCACTCAGCT-3'). All targeted clones were confirmed by Southern blot analysis using a cDNA probe containing exons 7-10. The targeted clones were injected into the C57BL/6J blastocysts, yielding two lines of chimeric mice which transmitted the floxed allele through the germ line.

Generation of liver specific HMGCR knockout mice.

Mice expressing Cre recombinase under the control of the albumin gene promoter (Alb-Cre) were kindly provided by Dr. D. LeRoith, W. Ogawa and M Kasuga as described in main text were backcrossed with C57BL/6J mice 6 times before interbreeding. $HMGCR^{+/f}$ carrying one copy of the Alb-Cre transgene were interbred with $HMGCR^{+/f}$ littermates lacking Cre to generate liver-specific HMGCR knock-out ($HMGCR^{f/f}$ Alb-Cre; L-HMGCRKO) mice and littermate control [$HMGCR^{f/f}$ (fHMGCR), $HMGCR^{+/+}$;Alb-Cre (CRE), and $HMGCR^{+/+}$ (WT)] mice. Age- and sex-matched littermates were used as the controls. Disruption of the floxed HMGCR allele in the mice was confirmed by Southern blot and Northern blot analyses. Genotyping was performed by PCR using genomic DNA isolated from the tail tip. The primer sequences for the Alb-Cre transgenes were as follows: primer A,5'GTGGTTAATGATCTACAG 3';primer B 5'CCTGAACATGTCCATCAG 3'.For floxed HMGCR genotyping, we used as primer A, 5' GTCGACGTTGAA TCCTCTTGTCAGAC 3'; and primer B, 5'CAAAGCAGACATGAGACTATTC 3'. All mice were group-housed in cages with a 12-hour light/dark cycle and fed CE-2 (Japan CLEA). Unless otherwise stated, they were fed a chow diet *ad libitum*, and tissues were collected in the early dark phase at a time when HMGCR activity was at its peak of diurnal rhythm[2].

Liver parenchymal and non-parenchymal cell isolation.

Liver parenchymal and non-parenchymal cells were isolated using the two-step liver perfusion method as described previously[3]. Because the parenchymal cells from L-HMGCRKO mice after 4 weeks of age were easy to die after perfusion with collagenase, L-HMGCRKO mice at 3 weeks of age were used. In brief, animals were anesthetized with pentobarbital sodium. Then, the abdominal cavity was opened, and the portal vein was cannulated using a 24-G elastic detention needle. The liver was perfused immediately with 20ml of the first perfusate (Ca 2+ free Hanks' balanced salt solution (HBSS) with 10 mM HEPES, 0.5 mM EGTA and 10 mM glucose, pH 7.4) at a flow rate of 6 ml/min to remove all of the blood. Outflow was performed by cutting the inferior vena cava. The perfusate was changed to 5ml of the second perfusate (HBSS containing 0.5mg/ml type IV collagenase (WAKO), type II trypsin inhibitor (Sigma), 5mM $CaCl_2$ and 10mM HEPES, pH 7.4). The second perfusion was at a same flow rate as the first perfusion. The liver was removed, transferred to a petri dish containing cold Williams E medium (GIBCO) supplemented with 5% fetal calf serum (FCS), and minced gently. Parenchymal and non-parenchymal components were prepared according to Rountree *et al.*[4]. In brief, the cells were centrifuged at 50 x *g* for 1 minute. The pellet was saved as parenchymal cell-enriched fraction. The supernatant was

centrifuged at 50 x *g* for 1 minute, and the supernatant centrifugation at 50 x *g* for 1 minute. The final supernatant was centrifuged at 180 x *g* for 8 minutes, with the pellet representing the non-parenchymal cell fraction (endothelial cells, Kupffer cells, stellate cells, and biliary cells). Total RNA was extracted from isolated non-parenchymal cells and used for quantitative real-time PCR. The first parenchymal cell-enriched pellet was further purified by density-gradient centrifugation in Percoll[5]. This technique reduces contamination of parenchymal cells by other cell types and by non-viable cells. After incubation in Williams E medium supplemented with 5% FCS for 3 hours, the attached parenchymal cells were subjected to total RNA extraction for quantitative real-time PCR or microsomal protein extraction for HMGCR activity assay.

Northern blot analysis and quantitative real-time PCR

Total RNA was prepared from mouse tissues or liver cells using TRIzol (Invitrogen). For the Northern blot analysis, pooled total RNA was subjected to 1% agarose gel electrophoresis in the presence of formalin and was transferred to Hybond N+ membranes (GE healthcare). The membranes were hybridized to ^{32}P-labeled HMGCR cDNA probes containing exons 2-4. Radioactivity was quantified with a BAS 2000 (Fujifilm). For Quantitative real-time PCR, all reactions were done in triplicate and relative amounts of mRNA were calculated using a standard curve or the comparative

CT method with the 7300 Real-Time PCR system (Applied Biosystems) according to the manufacturer's protocol. Mouse β actin mRNA was used as the invariant control. The primer-probe sets for real-time PCR are listed in supplemental table I.

Immunoblot analyses of liver cytosolic and membranous fractions.

To prepare cytosolic and membranous fractions for immunoblot analyses, aliquots of frozen liver (~100 mg) were homogenized in 1 ml of buffer (20mM Tris-Cl at pH 7.4, 2mM MgCl2, 0.25M sucrose, 10mM sodium EDTA, and 10-mM sodium EGTA) supplemented with a protease inhibitor cocktail (Sigma). The liver homogenate was centrifuged at 1,000 x *g* for 5 min at 4°C. The supernatant was removed and used to prepare membranous and cytosolic fractions as described previously[6]. After aliquots of the cytosolic and membranous fraction were removed for measuring protein concentrations with the BCA Kit (Pierce Biotechnology), the remainder from each protein (45 μg) was subjected to SDS-PAGE and immunoblotting. For immunoblot analysis of apolipoprotein B, 2μl of plasma were delipidated and subjected to 3~8% SDS-PAGE. Rabbit polyclonal antibody that detect mouse HMGCR[7] was kindly provided by Dr.YK Ho, MS Brown and JL Goldstein. Addional antibodies used include as follows: LDL receptor antibody (R and D Systems), apolipoprotein B (Santa Cruz Biotechnology), H-ras, pan-Akt, pan-Akt (phospho T308), STAT3, STAT3 (phospho

Y705) and c-Met (Abcam), Rac1 (Upstate Biotechnology), GAPDH (Ambion) and transferrin receptor (Zymed Laboratories).

HMGCR activity assay

HMGCR activity in the liver microsomal fraction was measured essentially as described previously (Ref. 9 in the main text). Briefly, the microsomal fraction (~50 μg) was incubated in 20 μl of a buffer containing 110 μM DL-[3-^{14}C] HMG-CoA (20 nCi/nmol), 5 mM NADPH, 10 mM EDTA, 10 mM dithiothreitol, and 100 mM potassium phosphate, pH 7.4, at 37 °C for 60 min. The reaction was terminated by the addition of 10 μl of 2 N HCl and incubation continued for another 30 min at 37 °C to lactonize the mevalonate formed. The [^{14}C] mevalonate was isolated by TLC and measured using [^{3}H] mevalonate as an internal standard. HMGCR activity is expressed as picomoles of [^{14}C] mevalonate formed per minute per mg of protein.

Lipids and biochemical analysis

Blood was drawn from the retro-orbital sinus; plasma was separated immediately and stored at –80°C. Blood glucose levels were measured with a FreeStyle blood glucose monitoring system (NIPRO). Concentrations of cholesterol, free cholesterol, cholesterol ester, triglycerides and free fatty acids in plasma and liver were measured as described (Ref.10 in the main text). The liver fatty acid contents were analyzed by

gas-liquid chromatography. Plasma AST, ALT and total bilirubin levels were measured with a kit from Wako Pure Chemical Industries.

HPLC analysis for plasma lipoprotein

Plasma lipoprotein profiles were analyzed using HPLC (Liposearch®; Skylight Biotech Inc., Tokyo, Japan) according to Okazaki *et al.*[8].

Lipoprotein X (Lp-X) detection

Lp-X was detected by eletrophoresis as described previously[9]. In brief, 1.5μl of fresh plasma was applied onto 1% agar gel and run in barbital buffer (pH 8.8) at 90 V for 25 min. Cholesterol was stained using a commercial reagent (Titan gel S-cholesterol, Helena laboratory).

Measurement of hepatic lipids synthesis in vitro using liver slices

Hepatic lipids synthesis was examined in vitro using liver slices as described elsewhere[10]. In brief, the animals were killed and the liver was immediately removed and chilled. Liver slices (~100 mg) were cut into small pieces and placed in 5.0 ml of Krebs' bicarbonate buffer (pH 7.4) containing 8 mM [2-^{14}C] acetate (0.1 μCi/μmol). The slices were then incubated 90 min at 37℃ at 120 oscillation/min. They were then saponified, and the nonsaponifiable sterols were isolated by TLC. After extraction of the non-saponifiable sterols and acidification with HCl, the ^{14}C-labeled fatty acids were extracted. The radioactivity of isolated sterols and fatty acids was measured. The results

were expressed as nmol/h/100 mg of liver wet weight.

Liver ceramide and diglyceride levels

Liver ceramide and diglyceride content levels were determined using the diglyceride kinase method as described previously[11]. In brief, liver was freeze-dried and dissected free of visible connective tissue. Lipids were extracted with chloroform:methanol:PBS (1:2:0.8). Diglyceride kinase (Calbiovhem) and γ-[^{32}P] ATP (10 mCi/mmol cold ATP) were added to lysates preincubated with β-octylglucoside and 1,2-dioleoyl-*sn*-glycero-3-phospho-1-glycerol. The reaction was stopped after 30 min by the addition of chloroform:methanol (2:1), and extracted lipids were spotted onto TLC plates and developed in chloroform:acetone: methanol:acetic acid:water (100:40:30:20:10). [^{32}P] phosphatidic acid (corresponding to diglyceride content) and ceramide-1-phosphate (corresponding to ceramide content) were identified and scraped from the TLC plate for scintillation counting.

Measurement of hydrogen peroxide (H_2O_2) levels

For determination of Hydrogen peroxide (H_2O_2) levels in the mouse liver, freshly harvested tissue was homogenized on ice and subsequently centrifuged at 12,000 x *g* for 10 min at 4°C. Total protein (10~20μg) from the supernatant was used to measure H_2O_2 by OxiSelect in Vitro ROS/RNS Assay kit (Cell biolab).

Measurement of caspase 3 and caspase 8 activity in vivo

For determination of caspase 3 and caspase 8 activity in the mouse liver, freshly harvested tissue was homogenized on ice and subsequently centrifuged at 12,000 ×*g* for 10 min at 4°C.Total protein (100 μg) from the supernatant was used to measure caspase activities by the ApoAlert caspase fluorescent-assay kit (CLONTECH).

Histological analyses

Livers were fixed in 10% neutral buffered formalin. Paraffin-embedded sections were stained with hematoxylin and eosin (HE) staining and TdT-mediated dUTP-biotin nick-end labeling (TUNEL). Ki-67 antibody which recognizes a nuclear protein associated with cell proliferation and type 4 collagen antibody which recognizes a liver fibrous structural protein. Frozen sections of liver tissue were stained with oil-red O and examined by light microscopy.

Mevalonate supplementation

Male (n=5) and female (n=5) L-HMGCR KO mice were given mevalonate (Sigma) in drinking water at a concentration of 5 mM from the age of 28 days to 35 days. The mice were then killed and blood and liver samples were collected and analyzed.

Male (n=8) and female (n=7) L-HMGCR KO mice were given mevalonate from the age

of 28 days to 40 days and their survival was observed.

Glucose supplementation

L-HMGCR KO mice were given D-glucose (WAKO) in drinking water at a concentration of 20% (w/v) from the age of 28 days to 40 days and their survival was observed. At the age of 35 days, the survivor's blood were collected and analyzed.

Statistics.

Statistical analyses were performed using Student's *t* test (2-tailed) as described in the Table legends. All calculations were performed with GraphPad Prism 4.0 software (GraphPad).

Supplemental References

1. Ishibashi S, Brown MS, Goldstein JL, Gerard RD, Hammer RE, Herz J. Hypercholesterolemia in low density lipoprotein receptor knockout mice and its reversal by adenovirus-mediated gene delivery. *J Clin Invest.* 1993;92:883-893
2. Hwa JJ, Zollman S, Warden CH, Taylor BA, Edwards PA, Fogelman AM, Lusis AJ. Genetic and dietary interactions in the regulation of HMG-CoA reductase gene expression. *J Lipid Res.* 1992;33:711-725
3. Sekiya M, Osuga J, Yahagi N, Okazaki H, Tamura Y, Igarashi M, Takase S,

Harada K, Okazaki S, Iizuka Y, Ohashi K, Yagyu H, Okazaki M, Gotoda T, Nagai R, Kadowaki T, Shimano H, Yamada N, Ishibashi S. Hormone-sensitive lipase is involved in hepatic cholesteryl ester hydrolysis. *J Lipid Res.* 2008;49:1829-1838

4. Rountree CB, Wang X, Ge S, Barsky L, Zhu J, Gonzales I, Crooks GM. Bone marrow fails to differentiate into liver epithelium during murine development and regeneration. *Hepatology.* 2007;45:1250-1260

5. Lee P, Peng H, Gelbart T, Beutler E. The IL-6- and lipopolysaccharide-induced transcription of hepcidin in HFE-, transferrin receptor 2-, and beta 2-microglobulin-deficient hepatocytes. *Proc Natl Acad Sci U S A.* 2004;101:9263-9265

6. Engelking LJ, Kuriyama H, Hammer RE, Horton JD, Brown MS, Goldstein JL, Liang G. Overexpression of Insig-1 in the livers of transgenic mice inhibits SREBP processing and reduces insulin-stimulated lipogenesis. *J Clin Invest.* 2004;113:1168-1175

7. Sato R, Goldstein JL, Brown MS. Replacement of serine-871 of hamster 3-hydroxy-3-methylglutaryl-CoA reductase prevents phosphorylation by AMP-activated kinase and blocks inhibition of sterol synthesis induced by ATP

depletion. *Proc Natl Acad Sci U S A.* 1993;90:9261-9265

8. Usui S, Hara Y, Hosaki S, Okazaki M. A new on-line dual enzymatic method for simultaneous quantification of cholesterol and triglycerides in lipoproteins by HPLC. *J Lipid Res.* 2002;43:805-814

9. Seidel D, Alaupovic P, Furman RH. A lipoprotein characterizing obstructive jaundice. I. Method for quantitative separation and identification of lipoproteins in jaundiced subjects. *J Clin Invest.* 1969;48:1211-1223

10. Andersen JM, Dietschy JM. Regulation of sterol synthesis in 16 tissues of rat. I. Effect of diurnal light cycling, fasting, stress, manipulation of enterohepatic circulation, and administration of chylomicrons and triton. *J Biol Chem.* 1977;252:3646-3651

11. Perry DK, Bielawska A, Hannun YA. Quantitative determination of ceramide using diglyceride kinase. *Methods Enzymol.* 2000;312:22-31

Supplemental table I

Real-time PCR primer/probe sequences.

gene	Forward primer	Reverse primer	Probe
SREBP1a	GGCCGAGATGTGCGAACT	TTGTTGATGAGCTGGAGCATGT	AGCGGTTTTGAACGACAT
SREBP1c	TGGATTGCACATTTGAAGACATG	GGCCCGGGAAGTCACTGT	CAGCTCATCAACAACCA
SREBP2	CCGGTCCTCCATCAACGA	TGGCATCTGTCCCCATGACT	AAAATCATAGAGTTGAAGGACT
LDL receptor	AGGCTGTGGGCTCCATAGG	TGCGGTCCAGGGTCATCT	TATCTGCTCTTCACCAACC
HMGCR	CGTCATTCATTTCCTCGACAAA	AGCAGAAAAAAGGGCAAAGCT	AACTGACAGGCTTAAAT
SS	CCAACTCAATGGGTCTGTTCCT	TGGCTTAGCAAAGTCTTCCAACT	CAGAAAACAAATATCATTCG
CYP7A1	AGCAACTAAACAACCTGCCAGTACTA	GTCCGGATATTCAAGGATGCA	CATCAAGGAGGCTCTG
ACC	GGACAGACTGATCGCAGAGAAAG	TGGAGAGCCCCACACACA	TGGCAGGAGATCGCAGT
FAS	GCTGCGGAAACTTCAGGAAAT	AGAGACGTGTCACTCCTGGACTT	ACTCGGCTACTGACACGA
SCD1	TCCGGAAATGAACGAGAGAAGGTGAAGA	AGATCTCCAGTTCTTACACGACCAC	GACGGATGTCTTCTTCCAGGTG
SCD2	GTGTCCAGGGCTGCTGTCTT	CACTCAGCCGCTCTTGCA	CCAGGATTAAGAGAACTGGA
DGAT1	TCCGCCTCTGGGCATTC	GAATCGGCCCACAATCCA	CCATGATGGCTCAGGTCCCACTGG
DGAT2	TGGAACACGCCCAAGAAAG	CACACGGCCCAGTTTCG	TGGCAGGAGATCGCAGT
MTP	GCTCCCTCAGCTGGTGGAT	CAGGATGGCTTCTAGCGAGTCT	ACCTCTGCTCAGACTC
LXRα	GCTCTGCTCATTGCCATCAG	TGTTGCAGCCTCTCTACTTGGA	CTGCAGACCGGCCCA
BAX	GGCCTTTTTGCTACAGGGTTT	GTGTCTCCCCAGCCATCCT	ATCCAGGATCGAGCAGG
Bcl2	ATCTTCTCCTTCCAGCCTGAGA	ACGTCCTGGCAGCCATGT	CAACCCAATGCCCG
CHOP	CATCCCCAGGAAACGAAGAG	GCTAGGGACGCAGGGTCAA	AAGAATCAAAAACCTTCACTACT
β actin	CGATGCCCTGAGGCTCTTT	TGGATGCCACAGGATTCCA	CCAGCCTTCCTTCTT

Legends for supplemental figures

Supplemental figure I

Targeting strategy and conditional deletion of HMGCR gene in mice.

Cre-mediated excision of the sequences between *loxP* sites deleted exons 2 to 4. The location of the probe used for Southern blot and Northern blot analysis is denoted by the

horizontal filled rectangle labeled "probe for Southern blot." or "probe for Nouthern blot".

Supplemental figure II

(A) Total RNA from the skin, intestine and adrenal which are the cholesterogenic organs of mice (n = 5 in each group) was subjected to quantitative real-time PCR for HMGCR gene expressions as described in Supplemental Methods. Each value represents the amount of mRNA relative to that in the control mice. (B) The HMGCR mRNA expression levels from the livers of surviver L-HMGCR KO mice at 14 weeks of age. Each value represents the amount of mRNA relative to that in the control mice, which is arbitrarily defined as 1 (n=3 in each group). Values are mean ± SD.

(C) The HMGCR mRNA expression level in isolated parenchymal cells and non-parenchymal cells at 3 weeks of age (n =9 in each group). Each value represents the amount of mRNA relative to that in the parenchymal cells from control mice, which is arbitrarily defined as 1. Values are mean ± SD. Significant differences compared with control mice: **, $P<0.001$. (D) The HMGCR activities in isolated parenchymal cells from the control and L-HMGCRKO mice at 3 weeks of age (n =9 in each group). Values are mean ± SD. Significant differences compared with control mice: *, $P<0.05$.

Supplemental figure III

Plasma lipoprotein profiles using HPLC analysis. The chromatographic patterns of mean value from control (gray line) and L-HMGCRKO (black line) at 3 weeks of age (A and B) and 5 weeks of age (C and D) are shown. Immunoblot analysis of plasma apolipoprotein (Apo) B (E, at 3 weeks; G, at 5 weeks of age) and Low density lipoprotein receptor (LDLR) (F, at 3 weeks; H at 5 weeks of age) of control and L-HMGCRKO mice are shown. The membrane protein transferrin receptor (TfR) was used as a loading control for LDLR protein levels. (I) Representative gel electrophoresis of Lipoprotein-X (Lp-X) is shown in an agar gel of plasma samples from human serum control, fHMGCR, and L-HMGCRKO mice. Plasma of L-HMGCRKO mice contains a characteristic band for Lp-X of cathodally migrating on agar gel, indicated by the arrow. O, Origin; +, anode side of gel; –, cathode side of gel.

Supplemental figure IV

HE stained liver section from control (A and C) and L-HMGCRKO (B and D) mice (A and B, 4 weeks of age; C and D, 14 weeks of age).

Supplemental figure V

The liver tissue lysates in control and L-HMGCRKO (n = 5 in each group) were used to measure caspase 3 (**A**), caspase 8 (**B**) activity and hydrogen peroxide (H_2O_2) levels which is reactive oxygen species (**C**) by fluorescent assay as described in Supplemental Methods. (**D**) Total RNA from the livers (n = 5 in each group) were subjected to quantitative real-time PCR for apoptosis-related gene expressions at 5 weeks of age as described in Supplemental Methods. Each value represents the amount of mRNA relative to that in the control mice, which is arbitrarily defined as 1 (A, B and D respectively). Values are mean ± SD. Significant differences compared with control mice: *, $P<0.05$.

Supplemental figure VI

Male (n=15) and female (n=13) L-HMGCR KO mice were given glucose from the age of 28 days to 40 days and the survival curves were generated by the Kaplan-Meier method.

Supplementary Figure I